International Journal of Modern Engineering Research (IJMER)
www.ijmer.com Vol.2, Issue.1, Jan-Feb 2012 pp-281-288 ISSN: 2249-6645

# Consequence of Corrosion on Dynamic Behaviour of Steel Bridge Members

**J.M.R.S. Appuhamy[1], M. Ohga[1], P. Chun[1] and P.B.R. Dissanayake[2]**
[1]Department of Civil & Environmental Engineering, Ehime University,
Bunkyo-cho 3, Matsuyama 790-8577, Japan
[2]Department of Civil Engineering, University of Peradeniya,
Peradeniya 20400, Sri Lanka

## ABSTRACT
**Deterioration of steel bridge infrastructures constitutes a major worldwide problem in transportation engineering and maintenance management industry. Corrosion and fatigue cracking may be the two most important types of damage in aging structures. Various kinds of failures and the need of expensive replacements may occur even though the amount of metal destroyed is quite small. One of the major harmful effects of corrosion is the reduction of metal thickness leading to loss of mechanical strength and structural failure, causing severe disastrous and hazardous injuries to people.**

**Furthermore, some recent earthquakes demonstrated the potential seismic vulnerability of some types of steel bridges. Corrosion and its effects can trigger the damages caused by earthquakes and it would be vital to understand the behavior of existing steel bridges which are corroding for decades in future severe seismic events. Therefore, this paper proposes a methodology to estimate the reduction of seismic strength capacities due to corrosion, which can be used to make rational decisions about the maintenance management plan of steel highway and railway infrastructures.**

***Keywords*** **– Corrosion, Earthquakes, Seismic resistance, Steel bridges, Maintenance management.**

## I. INTRODUCTION
As bridges are regarded as critical components of a transport network, the safety of bridges is crucial to people's daily life and to the national economy. Steel girder bridges, like other structures, deteriorate over time due to environmental effects, material fatigue and overloading. As a consequence, their closure or traffic capacity reduction causes major inconveniences for the users and result in significant losses to the economy. Furthermore, major steel bridges are rather costly to construct, maintain and rehabilitate. Therefore, the design, maintenance, management and rehabilitation of this kind of structures are complex and challenging tasks. Consequently, they have to be performed using state-of-the-art technical solutions and the best practice gained over many years of experience.

Exposure of a steel structure to the natural environment and inadequate maintenance will cause corrosion. Corrosion is one of the most important causes of deterioration of steel girder bridges which affects their long term mechanical performance, usability and durability [1, 2]. It has been pointed out that the corrosion can lead to cracking (fracture), yielding or buckling of members which can result in stress concentration, changes in geometric parameters and a build-up of the corrosion products. These parameters are critical for the member's ability to resist load effects [3]. Further, it is known that the corrosion wastage and stress concentration caused by the surface irregularity of the corroded steel plates influence the remaining strength of corroded steel plates [4]. Controlling corrosion on bridge structures can prevent premature failure and lengthen their useful service life, both of which save money and natural resources, and promote public safety. Therefore, careful evaluation of remaining load-carrying capacities of corroded steel structures is of high importance in transportation and maintenance engineering.

Efficient maintenance, repair and rehabilitation of existing bridges require the development of a methodology that allows for an accurate evaluation of the load carrying capacity and prediction of remaining life. In the past few decades, several experimental studies and detailed investigations of corroded surfaces were done by some researchers in order to introduce methods of estimating the remaining strength capacities of corroded steel plates [5 - 8]. Recent worldwide severe earthquakes have shown that steel bridges can be vulnerable. Especially during the Great Hanshin Earthquake of January 17, 1995, steel bridge structures suffered various kinds of damages which they never experienced before [9]. Furthermore, many collapses, superstructure failures and joint failures were observed in San Francisco due to the Loma Prieta Earthquake on October 17, 1989 [10]. Therefore it is evident that the failure risk associated with severe corrosion of steel bridge structure under mega earthquake events could not be underestimated.

Despite these uncertainties and variations, one can learn from past earthquake damage, because many types of damage occur repeatedly. By being aware of typical vulnerabilities that bridges have experienced, it is possible to gain insight into structural behavior and to identify potential weaknesses

in existing and new bridges. Historically, observed damage has provided the impetus for many improvements in earthquake engineering codes and practice. Although there is no published information on the seismic performance of severely corroded members, practicing engineers have apparently not questioned whether rusted members can still exhibit the dynamic behavior and hysteretic energy dissipation capacity commonly relied on for seismic resistance [11, 12]. Therefore this paper aims to investigate the effect of severe corrosion on the remaining seismic capacities of existing steel bridge infrastructures.

## II. PRELIMINARY INVESTIGATION

A steel girder bridge of Ananai River in Kochi prefecture on the shoreline of the Pacific Ocean, which had been used for about hundred years, was used for this study. This bridge had simply supported steel plate girders with six spans, with each of 13.5 m. It was constructed as a railway bridge in 1900, and in 1975 changed to a pedestrian bridge, when the reinforced concrete slab was cast on main girders. The bridge was dismantled due to serious corrosion damage in year 2001.

### 2.1 Corroded Specimens for Tensile Test

The specimens for tensile loading tests were cut out from the portion adjacent to end support of a plate girder of Ananai River Bridge. There, 21 flange specimens (F1-F21) and 5 web specimens (W1-W5) were fabricated from the cover plate on upper flange and web plate respectively. Here, the flange and web specimens have the widths ranged from 70-80mm and 170-180mm respectively. Test specimen configuration is shown in Figure 1.

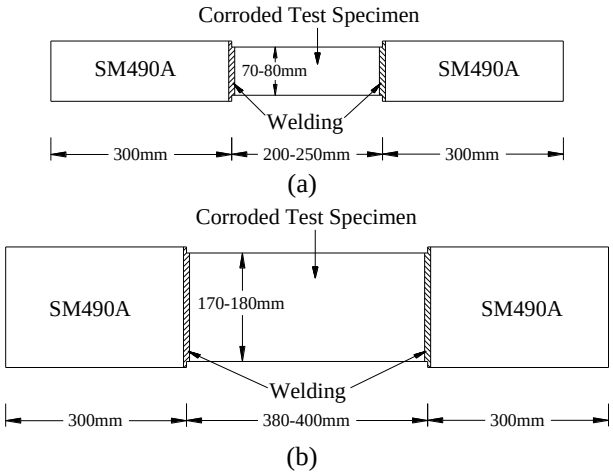


Fig. 1: Dimensions of (a) flange and (b) web test specimens

In addition, 4 corrosion-free specimens (JIS5 type) were made of each two from flange and web, and the tensile tests were carried out in order to clarify the material properties of test specimens. The material properties obtained from these tests are shown in Table 1.

Table 1: Material properties

| Specimen | Elastic modulus /(GPa) | Poisson's ratio | Yield stress /(MPa) | Tensile strength /(MPa) | Elongation at breaking /(%) |
|---|---|---|---|---|---|
| Corrosion-free plate (flange) | 187.8 | 0.271 | 281.6 | 431.3 | 40.19 |
| Corrosion-free plate (web) | 195.4 | 0.281 | 307.8 | 463.5 | 32.87 |
| SS400 JIS | 200.0 | 0.300 | 245~ | 400~510 | – |

### 2.2 Classification of Corrosion Levels

In this study, all specimens were categorized into typical 3 corrosion types concerning their corrosion conditions and minimum thickness ratio, μ (minimum thickness/ initial thickness). Figure 2 shows the relationship between the nominal ultimate stress ratio ($\sigma_{bn}/\sigma_b$) and the minimum thickness ratio (μ), where $\sigma_{bn}$ is the nominal ultimate stress and $\sigma_b$ is the ultimate stress of corrosion-free plate.

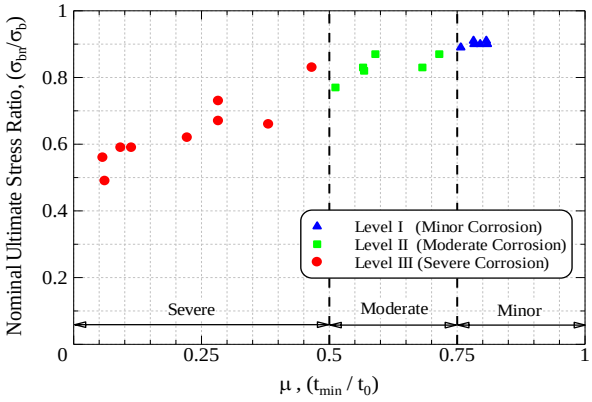


Fig. 2: Relationship of ultimate stress ratio & minimum thickness ratio (μ)

The corrosion conditions with the minimum thickness ratio, $\mu > 0.75$ are defined as 'minor corrosion'. And the 'moderate corrosion' type is defined when the minimum thickness ratio, $0.75 \geq \mu \geq 0.5$. Further, the 3rd corrosion type with the minimum thickness ratio, $\mu < 0.5$ is defined as 'severe corrosion' [8]. There, the initial thickness ($t_0$) of flange and web specimens are 10.5mm and10.0mm.

### 2.3 Numerical Analysis

The non-linear finite element analyses were performed for the specimens with different corrosion conditions in order to clarify the yield and tensile strengths, failure surfaces and the ultimate behaviors of corroded members. The 3D isoparametric hexahedral solid element with eight nodal points (HX8M) and updated Lagrangian method based on incremental theory were adopted in these analyses. Non linear elastic-plastic material, Newton-Raphson flow rule and Von Mises yield criterion were assumed for material

properties. Further, an automatic incremental-iterative solution procedure was performed until they reached to the pre-defined termination limit.

The analytical models with different length (L) and width (W) dimensions were modeled with their respective corrosion conditions and 2mm regular mesh pattern was adopted for all analytical models. One edge of the member's translation in X, Y and Z directions were fixed and only the Y and Z direction translations of the other edge (loading edge) were fixed to simulate with the actual experimental condition. Then the uniform incremental displacements were applied to the loading edge. Yield stress $\sigma_y$ = 294.7 [MPa], Elastic modulus E = 191.6 [GPa], Poisson's ratio ν = 0.276 were applied to all analytical models, respectively.

### *2.3.1 Ductile Fracture Criterion*

The "Stress Modified Critical Strain Model (SMCS)" was proposed by Kavinde *et al.* [13], to evaluate the initiation of ductile fracture as a function of multiaxial plastic strains and stresses. This method was adopted in this analytical study. In SMCS criterion, the critical plastic strain ($\varepsilon_p^{critical}$) is determined by the following expression:

$$\varepsilon_P^{Critical} = \alpha \cdot Exp\left(-1.5\frac{\sigma_m}{\sigma_e}\right) \qquad (1)$$

Where, α is toughness index and the stress triaxiality T = ($\sigma_m/\sigma_e$), a ratio of the mean or hydrostatic stress ($\sigma_m$) and the effective or von Mises stress ($\sigma_e$). The toughness index α is a fundamental material property and hence obtained from the tensile test conducted for the non corroded specimen and obtained as follows:

$$\alpha = \frac{\varepsilon_P^{Critical}}{Exp\left(-1.5\frac{\sigma_m}{\sigma_e}\right)} \qquad (2)$$

The ultimate strength of each corroded specimen was calculated accordingly by using the SMCS criterion and compared with their experimental ultimate capacities to understand the feasibility of the numerical modeling approach for remaining strength estimation of corroded steel plates with different corrosion conditions.

### *2.3.2 Analytical Results*

First, analytical modeling of the non-corroded specimen was done with above described modeling and analytical features to understand the accuracy of the adopted procedure. It was found that the analytical model results were almost same as the experimental results with having a negligible percentage error of 0.03% and 0.02% in yield and tensile strengths respectively. Then, all other experimentally successful specimens were modeled accordingly and their yield and ultimate strengths were compared with the experimentally obtained values.

Figure 3 shows the comparison of experimental and analytical the load-displacement curves of three specimens F-14, F-13 and F-19 with minor, moderate and severe corrosion conditions respectively. There, it can be seen that a very good agreement of experimental and analytical load-displacement behaviors for all 3 classified corrosion types can be obtained. Here, the percentage errors in yield and tensile strength predictions of the analytical models of three corrosion types are 0.53% and 0.03% in F-14, 2.96% and 0.70% in F-13 and 3.20% and 5.53% in F-19 respectively. Therefore, it is revealed that this analytical method is accurate enough and hence can be used to predict the yield, tensile and dynamic behaviors of actual corroded specimens more precisely.

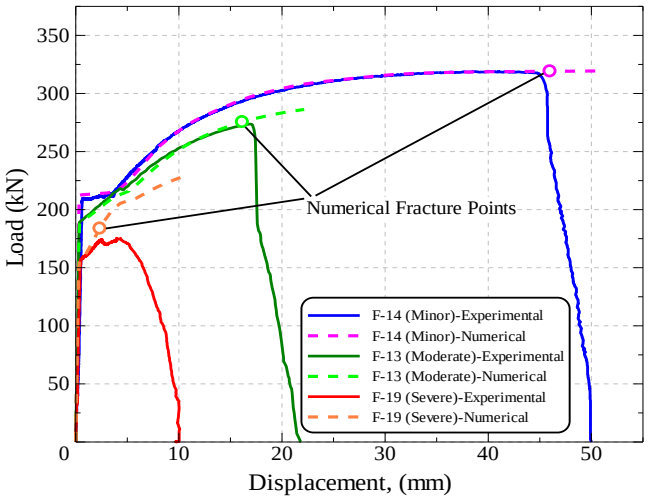


Fig. 3: Comparison of experimental and analytical load-displacement curves

### 2.4 Modeling of Corrosion Conditions

Two corrosion condition modeling (CCM) parameters were defined to model the corroded surface considering the material loss due to corrosion and stress concentration effect [14]. Figure 4(a) shows the variation of diameter of the maximum corroded pit (D) vs. maximum corroded depth ($t_{c,max}$) and Figure 4(b) shows the normalized average thickness ($t_{avg}/t_0$) vs. normalized maximum corroded depth ($t_{c,max}/t_0$). Both figures show a very good linear relationship and hence these parameters were used to develop an analytical model which can be used to predict the yield, ultimate and dynamic behaviors of corroded steel plates with different corrosion conditions.

Therefore, by considering the Figures 4(a) and (b), the two equations for the corrosion condition modeling (CCM) parameters can be defined as:

$$D^* = 5.2\ t_{c,max} \qquad (3)$$

$$t^*_{avg} = t_0 - 0.2\ t_{c,max} \qquad (4)$$

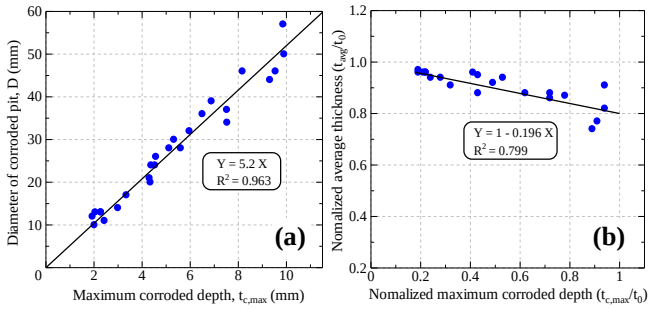


Fig. 4: Relationship of (a) D vs. $t_{c,max}$ and (b) normalized $t_{avg}$ vs. $t_{c,max}$

Where $D^*$ and $t^*_{avg}$ are the representative diameter of maximum corroded pit and representative average thickness respectively.

Figure 5 shows the analytical model, which is developed with the above CCM parameters with different corrosion conditions. Here, the maximum corroded pit was modeled with the representative diameter ($D^*$) which could account the stress concentration effect and the material loss due to corrosion was considered by using the representative average thickness parameter ($t^*_{avg}$). The same modeling features and analytical procedure as described in section 2.3 were adopted for the analyses.

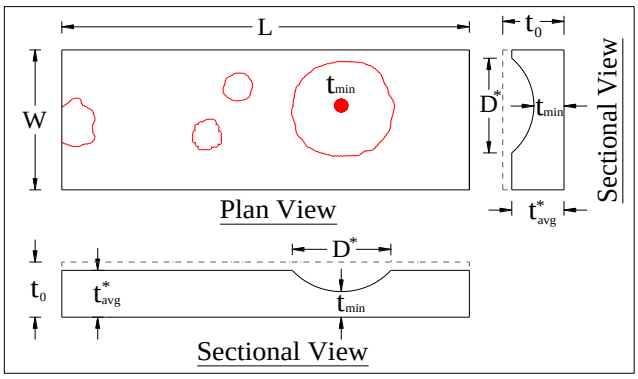


Fig. 5: Analytical model with CCM parameters

Figure 6 shows the comparison of load-displacement behavior of experimental and analytical results with proposed model for 3 members F-14, F-13 and F-19 with minor, moderate and severe corrosion conditions respectively. It was revealed that a very good comparison of the load-displacement behavior can be seen for the all three classified corrosion types for the proposed analytical model too. Here, the percentage errors in yield and tensile strength predictions of the proposed analytical model for the three corrosion types are 0.13% and 0.83% in F-14, 0.38% and 1.01% in F-13 and 3.51% and 2.69% in F-19 respectively.

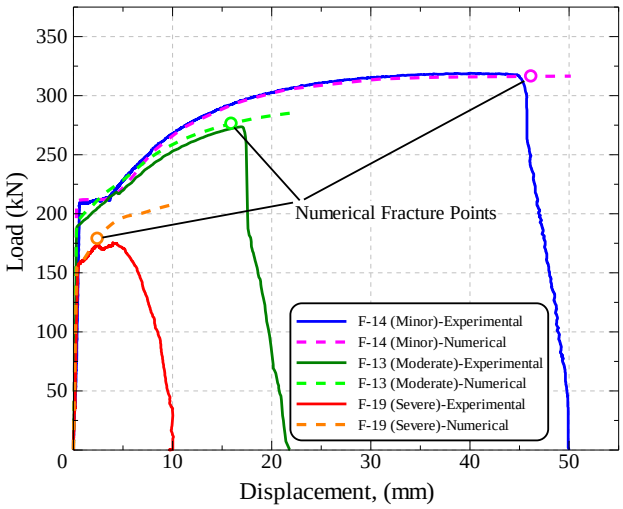


Fig. 6: Comparison of experimental and analytical load-displacement curves with proposed analytical model with CCM parameters

Then, all experimentally successful specimens were modeled accordingly with the proposed analytical model and their yield and ultimate strengths and failure surfaces were compared with the experimental results. Figure 7 shows the comparison of ultimate load capacities of all specimens in experimental and numerical analyses with proposed model with CCM parameters. Here, having a coefficient of correlation of $R^2$ = 0.992 indicate the accuracy of the proposed model and the possibility of the use of proposed analytical model instead of the model with detailed corroded surface measurements.

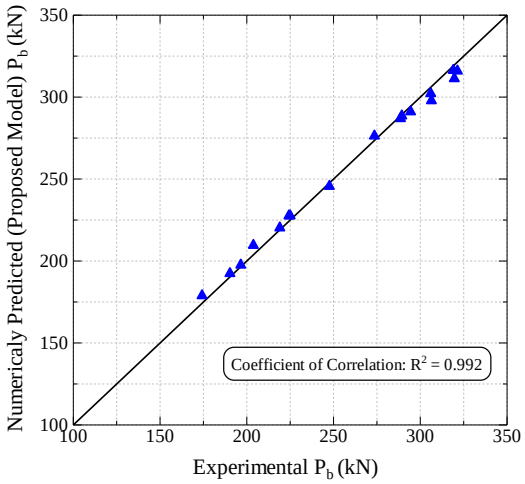


Fig. 7: Comparison of experimental and analytical ultimate load capacities with proposed analytical model with CCM parameters

## III. DYNAMIC ANALYSIS

The seismic capacity of existing bridges is important after an earthquake both to provide emergency supplies and transportation to society as well as to ensure structural safety in engineering terms. Better seismic capacity of bridges results in less structural damage and reduced impacts following an earthquake disaster. Therefore, an evaluation of the seismic capacity for numerous existing bridge inventories can be regarded as a fundamental basis for mitigating future losses caused by earthquakes.

### 3.1 Seismic Analysis with Historical Earthquakes

In this study, three major historical earthquake records were used to understand the dynamic response of Ananai River Bridge in Kochi prefecture, Japan. The seismic analyses were performed considering the earthquake excitations caused by; 1995 Kobe earthquake ($M_w$=6.9), 1989 Loma Prieta earthquake ($M_w$=6.9) and 1940 El-Centro earthquake ($M_w$=7.1). Figure 8 shows the acceleration histories of 1995 Kobe earthquake used in this analysis.

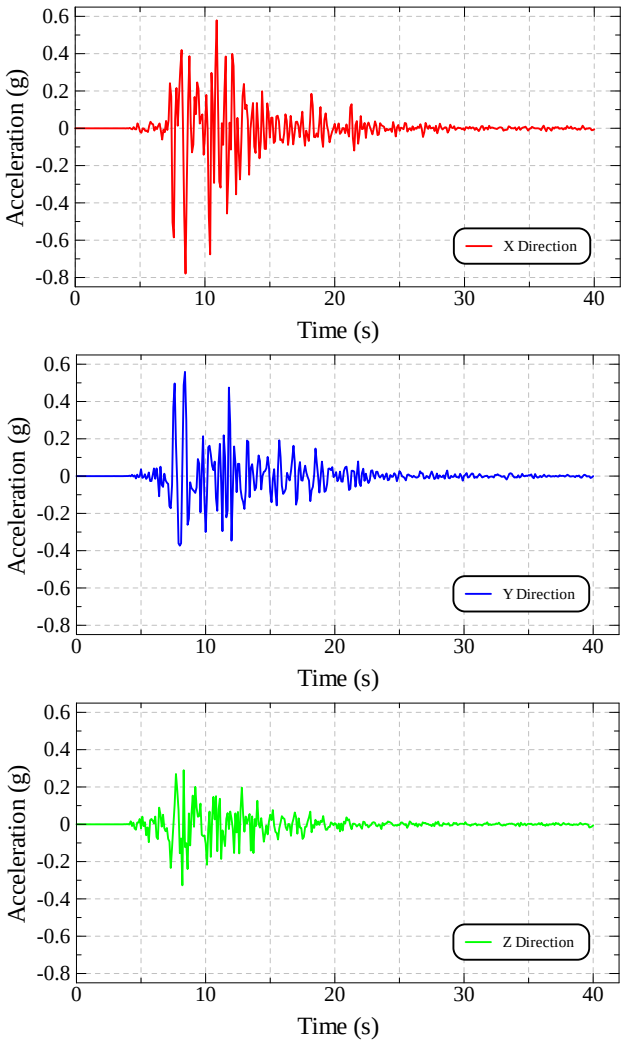


Fig. 8: Acceleration histories of 1995 Kobe earthquake

The seismic response analysis is performed in two distinct stages. A natural frequency analysis is performed first. This is used to calculate the first 100 (or more; until more than 90% of total mass participation occurs) natural modes of vibration of the structure. The eigenvalues (frequencies) and eigenvectors (mode shapes) are stored and used in the subsequent IMDPlus analysis. The second phase of the analysis utilizes the IMDPlus option which performs enhanced time domain solutions using Interactive Modal Dynamics (IMD). In the IMDPlus solution, the structure is subjected to a support condition excitation governed by time histories of acceleration in the model global axes. In this example, the seismic excitation is applied directly to the bases of the structure using the first 40 seconds of each earthquake.

### 3.2 Results of Primary Seismic Analysis

The primary seismic analysis was performed with the three historical earthquakes as described above and the behavior of the structure was studied. In each analysis, critical members were identified considering the whole excitations of the corresponding earthquake records. It was noticed that, even though the main steel girders are well behaved due to earthquake loading, cross girder members were deformed in transverse direction. One example of the ultimate stress distribution of the bridge structure and the displacement history obtained for the critical member for the seismic analysis of 1995 Kobe earthquake is shown in Figure 9.

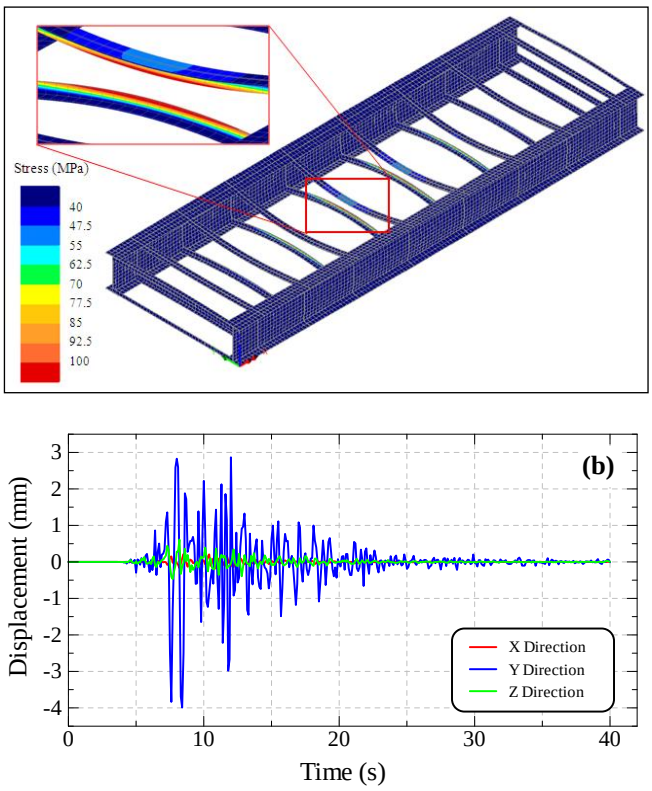


Fig. 9: (a) Ultimate stress distribution of steel girder and (b) displacement histories of the critical member [Kobe eqk.]

### 3.3 Secondary Seismic Analysis

#### *3.3.1 Analytical Models*

Five different analytical models were developed and analyzed with the same modeling features, analytical procedure, in order to understand the seismic strength deterioration with the severity of corrosion condition. Here, the seismic model SM-1 with μ=1 represents the model without corrosion and used as the standard model in this analysis to compare with other SM models. The different corrosion conditions were adopted by using different minimum thickness ratio (μ) values and the CCM parameters; representative diameter ($D^*$) and representative average thickness parameter ($t^*_{avg}$), were used to model the stress concentraion effect and material loss due to corrosion as decribbed in section 2.4. The details of those analytical models which are considered for this parametric study are shown in Table 2. The initial thickness ($t_0$) of the different sismic models (SM) was considered as 10.5mm. Here, the maximum corroded depth ($t_{c,max}$) can be expressed as follows:

$$\mu = \frac{t_{min}}{t_0} = \frac{(t_0 - t_{c,max})}{t_0}$$

$$t_{c,max} = t_0(1 - \mu) \qquad (5)$$

Table 2: Details of analytical models

| Model | μ ($t_{min}/t_0$) | $t_{c,max}$ (mm) | $D^*$ (mm) | $t^*_{avg}$ (mm) |
|---|---|---|---|---|
| SM-1 | 1.0 | 0.0 | 0.0 | 10.5 |
| SM-2 | 0.75 | 2.63 | 13.65 | 9.98 |
| SM-3 | 0.50 | 5.25 | 27.30 | 9.45 |
| SM-4 | 0.25 | 7.88 | 40.95 | 8.93 |
| SM-5 | 0.05 | 9.98 | 51.87 | 8.51 |

#### *3.3.2 Analytical Results*

The secondary seismic analysis for each seismic model (SM-1~SM-5) with different corrosion conditions, was performed by using the primary displacement histories obtained for each historical earthquake. The analyses were conducted until they reached to their pre-defined termination limits and the load-displacement behavior for each model was obtained.

Figure 10 shows the load-displacement curves for; (a) Kobe earthquake, (b) Loma Prieta earthquake and (c) El-Centro earthquake for each seismic model. They clearly show that the dynamic behavior of each model was affected by different corrosion conditions. Further, it was noted that their residual strengths were significantly affected by the different levels of corrosion conditions attributed to each SM model.

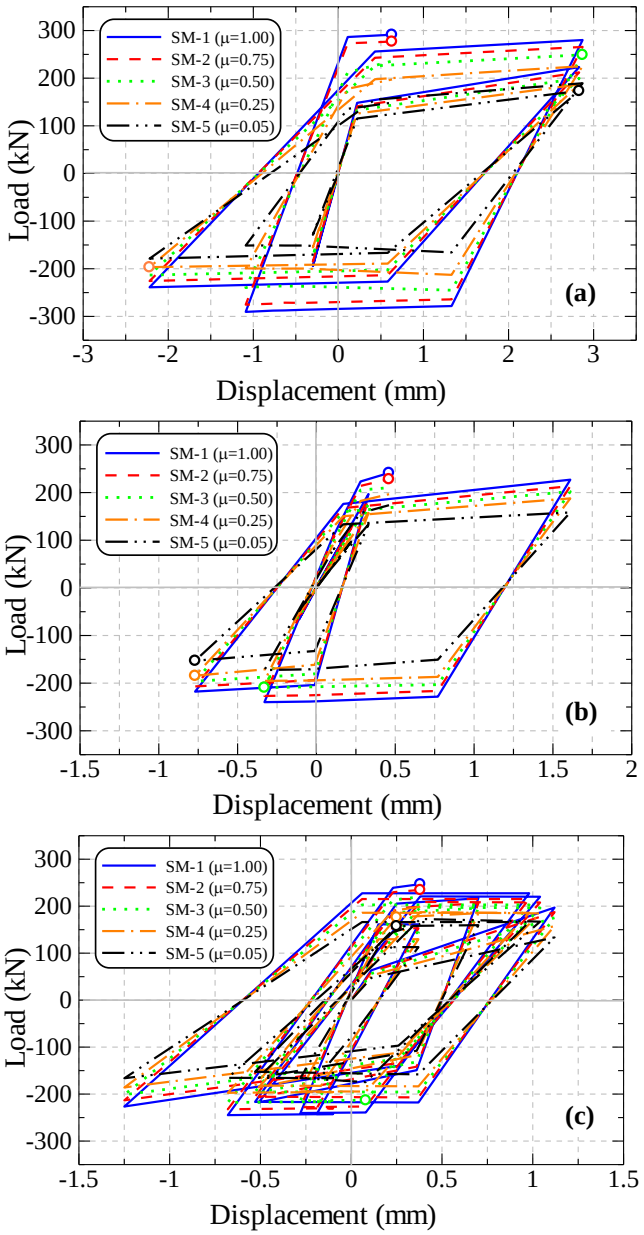


Fig. 10: Comparison of load-displacement curves of different seismic models for (a) Kobe earthquake, (b) Loma Prieta earthquake and (c) El-Centro earthquake

### 3.4 Discussion

The percentage seismic strength reductions (SSR%) in yield and ultimate strength states of each SM model are shown in Figure 11(a) and 11(b) respectively. There, the percentage strength reduction results of different seismic models and analytical results of tensile specimens developed with CCM parameters are shown. It was noted that percentage strength reductions (%SR) of tensile analysis have linear relationship in both yield and ultimate strength estimations. But it was noted that the %SSR in yield and ultimate states are non-linearly increased with increase of corrosion levels.

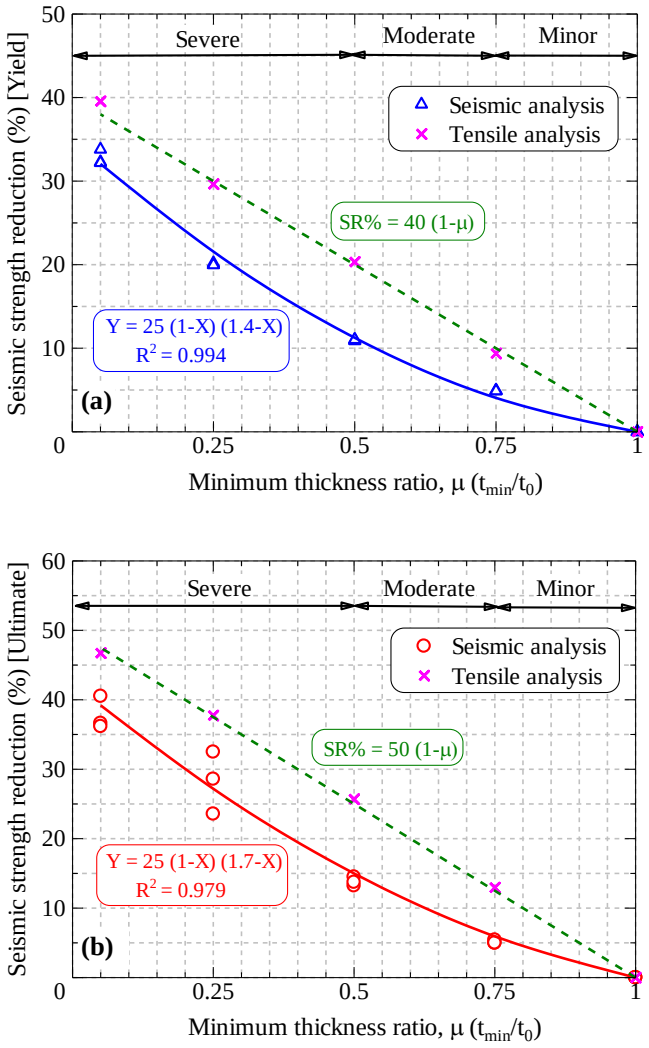


Fig. 11: Relationship of percentage (a) yield; (b) ultimate, seismic strength reduction vs. minimum thickness ratio (μ)

The remaining yield and ultimate seismic strength capacities are decreased with the severity of corrosion condition for all three different earthquake loading histories. Furthermore, these results divulged that having a corrosion pit of minimum thickness ratio μ=0.05, could reduce up to 30% ~ 40% of its' original yield and ultimate strengths respectively. It is noted from Figure 11 that two very good relationships can be obtained for remaining yield and ultimate seismic strength capacities with high accuracy. Therefore, by considering Figure 11(a) and 11(b), two equations for estimating remaining yield and ultimate seismic strength capacities can be derived as:

$$\%SSR_{yield} = 25\ (1-\mu)\ (1.4-\mu) \quad (6)$$

$$\%SSR_{ultimate} = 25\ (1-\mu)\ (1.7-\mu) \quad (7)$$

As the proposed strength reduction equations only requires the measurement of minimum thickness ratio, μ (minimum thickness/ initial thickness), which is an easily measurable parameter through a quick and careful site investigation, this method can be used as a simple and reliable method to predict the yield and ultimate seismic behaviors of corroded steel members more easily and precisely. Furthermore, the seismic strength reduction charts give a good indication about the % strength reduction according to the severity of corrosion and hence bridge engineers would be able to quickly decide the required maintenance works of corroded members, in order to assure the adequate safety of the infrastructure.

## IV. CONCLUSIONS

The corroded surface measurements and tensile tests were conducted on many wide specimens with different corrosion conditions, which are obtained from a plate girder which had been used for about 100 years with severe corrosion. Non-linear FEM analysis was carried out to understand the mechanical behavior, stress distribution, ultimate behavior etc. for members with different corroded conditions. The yield and ultimate behaviors of steel bridge members with different corrosion conditions were studied under different earthquake loadings. The main conclusions obtained from this study can be summarized as follows.

1. A very good agreement between experimental and non linear FEM results can be seen for all three classified corrosion types. So, the adopted numerical modeling technique can be used to predict the remaining strength capacities of actual corroded members accurately.
2. Even though, the steel main girders behave well during severe earthquakes, some types of transverse members could become critical and hence could suffer various structural damages.
3. Furthermore, the corrosion and its stress concentration effect will trigger those damages significant and could even lead to the collapse of total structure.
4. The percentage reduction of yield and ultimate strength capacities due to corrosion, under earthquake loadings can be defined as:

$$\%SSR_{yield} = 25\ (1-\mu)\ (1.4-\mu)$$

$$\%SSR_{ultimate} = 25\ (1-\mu)\ (1.7-\mu)$$

As the above equations have only a single variable, minimum thickness ratio (μ), which is an easily measurable parameter, it will reduce the contribution of the errors occurred during the practical investigation of a corroded member. Further this method is simple and hence can be used for the maintenance management of steel bridge infrastructures with better accuracy.

## REFERENCES

[1] K. Fujii, T. Kaita, H. Nakamura and M. Okumura, A model generating surface irregularities of corroded steel plate for analysis of remaining strength in bridge maintenance, *Proceedings of EASEC-9*, Indonesia, 9, 2003, 32-38.

[2] R. Rahgozar, Remaining capacity assessment of corrosion damaged beams using minimum curves, *Journal of Constructional Steel Research*, 65, 2009, 299-307.

[3] Y. Sharifi and R. Rahgozar, Remaining moment capacity of corroded steel beams, *International Journal of Steel Structures*, 10(2), 2010, 165-176.

[4] A. Kariya, K. Tagaya, T. Kaita and K. Fujii, Mechanical properties of corroded steel plate under tensile force, *Proceedings of the 3rd International Structural Engineering and Construction Conference*, Japan, 2005, 105-110.

[5] M. Matsumoto, Y. Shirai, I. Nakamura and N. Shiraishi, A proposal of effective thickness estimation method of corroded steel member, *Bridge and Foundation Engineering*, 23(12), 1989, 19-25. (in Japanese)

[6] A. Muranaka, O. Minata and K. Fujii, Estimation of residual strength and surface irregularity of the corroded steel plates, *Journal of Structural Engineering*, 44A, 1998, 1063-1071. (in Japanese)

[7] A. Kariya, K. Tagaya, T. Kaita and K. Fujii, Basic study on effective thickness of corroded steel plate and material property, *Annual Conference of JSCE*, Japan, 2003, 967-968. (in Japanese)

[8] J.M.R.S. Appuhamy, T. Kaita, M. Ohga and K. Fujii, Prediction of residual strength of corroded tensile steel plates, *International Journal of Steel Structures*, 11(1), 2011, 65-79.

[9] C. Miki and E. Sasaki, Fracture in steel bridge piers due to earthquakes, *International Journal of Steel Structures*, 5(2), 2005, 133-140.

[10] J.P. Moehle and M.O. Eberhard, Earthquake damage to bridges, *Bridge Engineering Handbook*, CRC Press, 2000, 1-34.

[11] M. Bruneau and S.M. Zahrai, Effect of severe corrosion on cyclic ductility of steel, *Journal of Structural Engineering*, 1997, 1478-1486.

[12] S.M. Zahrai, Cyclic strength and ductility of rusted steel members, *Asian Journal of Civil Engineering*, 4(2-4), 2003, 135-148.

[13] A.M. Kavinde and G.G. Deierlein, Void growth model and stress modified critical strain model to predict ductile fracture in structural steels, *Journal of Structural Engineering*, 132(12), 2006, 1907-1918.

[14] J.M.R.S. Appuhamy, M. Ohga, T. Kaita and P.B.R. Dissanayake, Reduction of ultimate strength due to corrosion - A finite element computational method, *International Journal of Engineering*, 5(2), 2011, 194-207.